Evaluation of a Triple-Axis Coherent Doppler Velocity Profiler for Measuring Near-Bed Flow: A Field Study

K. F. E. BETTERIDGE, P. S. BELL, P. D. THORNE, AND J. J. WILLIAMS

Proudman Oceanographic Laboratory, Liverpool, United Kingdom

(Manuscript received 19 May 2004, in final form 13 May 2005)

ABSTRACT

Collocated detailed measurements of near-bed turbulent and intrawave flow are important for studying sediment transport processes and seabed evolution. Existing commercially available triple-axis profiling instruments do not provide collocated velocity measurements. To improve the capability to make such measurements a triple-axis coherent Doppler velocity profiler (CDVP) has been developed and tested in the marine environment. The instrument was designed to measure orthogonal velocity profiles within a narrow column of water at 16 Hz within 1 m of the bed with a vertical spatial resolution of 0.05 m. This paper describes the first deployment of the instrument, in a tidal inlet in Portugal during a multidisciplinary study, when CDVP flow velocity measurements were compared with data from other instrumentation. A pragmatic approach was adopted to assess the capability of the triple-axis CDVP, using both an evaluation of internal consistency and an assessment against two commercially available acoustic Doppler velocimeters (ADVs). Measurements of the mean and fluctuating velocity profiles were collected with the triple-axis CDVP, and these have been shown to be internally consistent and to be in good agreement with measurements obtained with the ADVs.

1. Introduction

To advance scientific understanding of sediment entrainment, hydrodynamics, and bedform evolution, instruments to study near-bed sediment transport processes are under continual development. Data from evolving systems provide assessments of mathematical models and formulas used in the prediction of sediment transport and bedform changes. The measurement of the flow field close to the bed is of central importance to understanding sediment transport processes. In particular, to examine the details of sediment entrainment, it is necessary to measure intrawave and near-bed turbulence. Acoustic instrumentation has been favored and continues to be developed because such measurements are largely nonintrusive, provide profiles with centimetric spatial resolution, and resolve turbulent time scales (Thorne and Hanes 2002; Zedel and Hay 1999).

Acoustic Doppler velocimeters (ADVs) have been available for over a decade for measuring the three components of turbulent flow (Voulgaris and Trowbridge 1998). Although a significant contribution to high-resolution measurements, they are limited to observations at one location in the water column. In contrast, uni-axial coherent Doppler velocity profilers (CDVPs) measure the radial component of the turbulent flow field over a range of up to 1.5 m with a resolution of the order of centimeters (Hardcastle 1994; Zedel et al. 1996; Zedel and Hay 1999; Veron and Melville 1999; Thorne and Taylor 2000; Betteridge et al. 2002). In these systems fluid velocities are determined from the rate of change of phase of consecutive acoustic signals backscattered from suspended sediments. The axial component of the flow profile may therefore be obtained; however, these systems have been limited to measuring the flow in a single direction.

It is desirable to measure profiles of orthogonal turbulent flow components, and one option is provided commercially (see information online at http://www.sontek.com). This instrument can provide 2-Hz three-axis velocity profiles in centimetric range cells. However, the system uses diverging beams and therefore does not provide collocated velocity profiles. This can be a serious shortcoming in many hydrodynamic and sediment processes studies. Therefore, triple-axis CDVPs are currently being developed to obtain collocated measurements of the three orthogonal compo-

Corresponding author address: K. F. E. Betteridge, Proudman Oceanographic Laboratory, 6 Brownlow St., Liverpool L3 5DA, United Kingdom.
E-mail: kfeb@pol.ac.uk

nents of flow. There is literature on the development and use of such technology in laboratory tests for marine applications (e.g., Hurther and Lemmin 1998, 2001; Rolland and Lemmin 1997; Zedel and Hay 2002; Wilson et al. 2000). Here we describe the development and first reported marine trial of a triple-axis CDVP developed using converging beams. This triple-axis coherent Doppler velocity profiler was designed and built to address the issues of obtaining nonintrusive high-spatial- and high-temporal-resolution three-axis collocated velocity profiles in the nearshore marine environment. The CDVP was deployed during a European-funded field study, with other proven current measuring instrumentation, and advantage was taken of this study to assess within a marine setting the development of the CDVP. The deployment was on an instrument package at the entrance to a tidal lagoon at Ria Formosa, Algarve, Portugal, during a multidisciplinary study to examine the interacting hydrodynamics and morphodynamics occurring at tidal inlet entrances and along coastlines (Williams et al. 2003b). There was a wave–current environment at the tidal inlet site, with strong currents measuring from 0.4 to 2 m s^{-1} and waves with significant height, $H_{s,}$ of around 0.75 m and period, T_p, of about 5 s. The seabed was composed of coarse sand. The instruments in the project were located on an instrument package deployed on a jack-up barge (Williams et al. 2003a).

The CDVP consisted of one transceiver and two passive receivers. These were configured to measure profiles of the three orthogonal components of the flow. The flow components obtained with the triple-axis CDVP were assessed in a simple pragmatic way, by comparison with measurements collected by two ADVs. Initially the mean, time-averaged velocities measured by the CDVP were compared with the mean velocities measured by the ADVs, and the outcome gave very comparable results. This was followed by detailed comparisons of the 16-Hz measurements of the flow by both the CDVP and ADV time series, power spectra, and statistics, and regression analysis was used to quantify the capability of the CDVP. The results show very comparable velocity measurements, although there are some differences associated with a spatial separation between the ADVs and CDVP measurement volumes and some shortcomings in the CDVP itself.

2. Methodology

a. Coherent Doppler

Measurements of the vertical profile of the backscattered signal were obtained within closely spaced range bins by range gating. The radial velocity was obtained from the rate of change of the phase of consecutive backscattered signals (Zedel et al. 1996; Veron and Melville 1999). The phase Ψ is given by

$$\Psi = \tan^{-1}\left[\frac{\langle I(t)Q(t+T) - I(t+T)Q(t)\rangle}{\langle Q(t)Q(t+T) + I(t)I(t+T)\rangle}\right], \qquad (1)$$

$$\mathrm{f_d} = \frac{\Psi}{2\pi \mathrm{T}}$$

where T is the delay between transmission pulses; $I(t)$ and $Q(t)$ are, respectively, the in-phase and quadrature components of the received signal; and $\langle\rangle$ represents an average over a number of consecutive pulse pairs. The Doppler frequency shift f_d is given by

$$f_d = \frac{\Psi}{2\pi T} \qquad (2)$$

and the radial velocity v_d by

$$v_d = \frac{cf_d}{2f_0}, \qquad (3)$$

where c is the sound velocity in water, and f_o is the transmit frequency. The return from the ith pulse at the maximum range must be received before pulse $(I + 1)$ is transmitted to obtain unambiguous range information. The rate of pulse transmission, the pulse repetition frequency (PRF) determines the maximum unaliased value of the Doppler frequency f_d, and the maximum range–velocity relationship is given by $r_m v_{\mathrm{dm}} \leq c^2/8f_0$, where r_m is the maximum range, and v_{dm} is the maximum unaliased velocity that may be measured.

An early version of the CDVP used a PRF of 512 Hz, which gave an unambiguous velocity range given by $V_{\max} = (f_{\mathrm{PRF}}c/f_0)/4$ of ± 0.36 m s^{-1}, based on a Doppler phase shift of $\pm\pi$, with $c = 1500$ m s^{-1} and $f_0 = 524$ kHz. For the flow velocities greater than this, the Doppler phase shift signal is aliased. Velocities considerably in excess of this are commonly experienced in oceanographic environments. Therefore, to overcome this limitation the triple-axis CDVP employed a dual-PRF approach (Lhermitte and Serafin 1984). Applying this technique, the present system used two interleaved PRFs of 512 and 409.6 Hz with a timing ratio of 5/4 to further extend this unambiguous range, by generating two Doppler shift frequencies, the combination of which provided a unique solution to the water velocity up to 4 times the unambiguous limit of the single 512-Hz PRF (i.e., ± 1.46 m s^{-1}) in the radial direction of each transducer.

The coherent Doppler system produced complex phase information on the backscattered acoustic signal by mixing the returning signal with in-phase (I) and quadrature (Q) signals derived from the transmitter oscillator. The hardware to carry out this complex demodulation was of in-house design (Hardcastle 1994), and the resulting I and Q components were sampled using a 16-bit PC-based analog-to-digital card sampling the I and Q signals simultaneously at 16 384 Hz. The resulting phase information contained in the components of the complex signal were used in a four-quadrant arctan algorithm to extract the Doppler phase shift as given by Eq. (1). The system was designed to produce velocity readings at 16 Hz, allowing time for 28 pulses to be transmitted with interleaved PRFs, or 14 pulse pairs for each PRF at each time step. Equation (1) was applied to the data from each PRF separately, generating two related Doppler phase shifts for each sixteenth-of-a-second sample. Assuming low noise data, the combination of these two Doppler phase shifts relates to a unique velocity up to the combined ambiguity limit of ± 1.46 m s^{-1}. The two Doppler phase shifts for the two PRFs were logged by the PC recording software at 16 Hz ready for dealiasing.

The dealiasing was realized in postprocessing software by trying all possible aliasing combinations and choosing the combination and hence the velocity that yielded the lowest velocity difference between the Doppler shifts from the two PRFs. If the data were perfect and noiseless, one of these combinations would yield identical velocities. In reality, there was noise on the signals, so spike-detection routines were also implemented to reduce instances of incorrect dealiasing. This dealiasing software was fully automatic, requiring no operator intervention. The resulting velocity values were further geometrically corrected to give orthogonal velocity components.

b. Triple-axis system

The triple-axis CDVP described here was designed to provide collocated vertical profiles of the three orthogonal components of the flow: streamwise (u), crosswise (v), and vertical (w) flow. The CDVP consisted of a vertically mounted, downward-looking narrow-beam disc transducer, Tz, which transmitted a short pulse. The backscattered signal was received on the downward-looking transducer and also by two passive receivers located at 90° to each other in the horizontal plane. The beam patterns for the two receiving transducers, shown in Fig. 1, were specified for the purpose of receiving the backscattered signal from the whole vertical range insonified by the downward-looking transducer. A diagram showing the CDVP transducer configuration is shown in Fig. 2. The vertical transducer, Tz, operated at 524 kHz and had a −3 dB beam angle of approximately 1°. The two passive receivers, Rx and Ry, were chosen to be resonant at 530 kHz and were located orthogonally to Tz in the same horizontal plane and at a distance of 0.585 m. They were rectangular transducers that were housed in anodized aluminum, encapsulated in polyurethane, and had nominal dimensions of 0.005 m in height and 0.05 m in width. As shown in Fig. 1, this gave receivers with fan-shaped beam patterns, with a −3 dB full beam angle of 46° in the vertical, and a horizontal −3 dB beam angle of 2.9°. Each transducer measured the radial velocity component derived from the backscattered sound as it propagated to the bed, thereby yielding collocated velocity profiles.

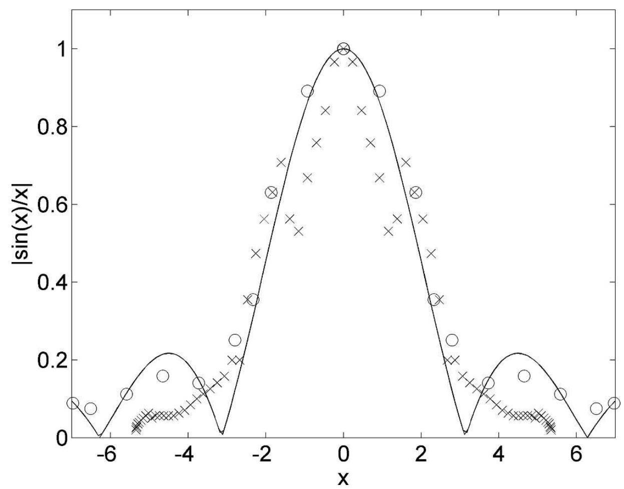

FIG. 1. The solid line shows $\sin(x)/x$ against x. This represents the beam pattern response for the rectangular aperture used in the two passive receivers in the present study. The variable x is given by $kL\sin\theta/2$, where L is the height or width of the radiating source. The measured responses of the receiver transducers are plotted for height L1 = 0.005 m (x) and width L2 = 0.05 m (o).

Referring to Fig. 2, the measured orthogonal flow velocities, u_m, v_m, and w_m, were obtained from the dealiased radial velocities V(Rx), V(Ry), and V(Tz) as follows. The velocity $\mathbf{V}$ is given by $\mathbf{V} = u_m\mathbf{i} + v_m\mathbf{j} + w_m\mathbf{k}$, where $\mathbf{i}$, $\mathbf{j}$, and $\mathbf{k}$ are the unit vectors in the three orthogonal directions, x, y, and z. The transceiver, Tz, measures the vertical flow component, w_m, directly. Receiver Ry was measuring components of v_m and w_m, and the radial velocity measured by Ry, V(Ry), is given by

$$V(\mathrm{Ry}) = v_m \cos\theta_y + w_m \sin\theta_y. \tag{4}$$

The crosswise flow velocity, v_m, may therefore be expressed as

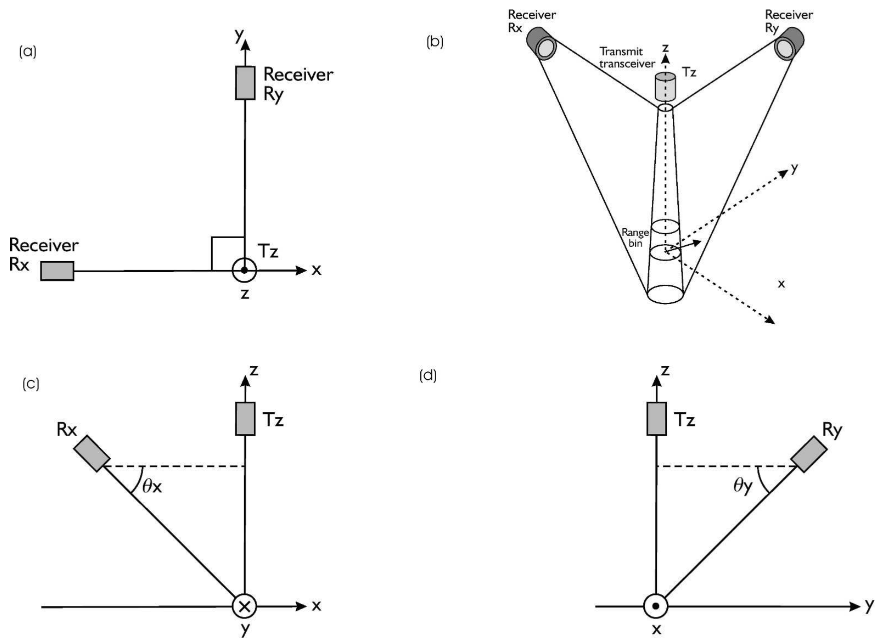

FIG. 2. (a), (c), (d) Projections of the relationships between the transducer locations and the volume insonified at one range bin in the x–y, x–z, and y–z planes, respectively. (b) The 3D impression of the arrangement.

$$V_m = \tan\theta_y[V(\mathrm{Ry})/\sin\theta_y - V(\mathrm{Tz})], \tag{5}$$

where $V(\mathrm{Tz}) = w_m$. For the streamwise flow component, u, from Rx and Tz,

$$V(\mathrm{Rx}) = -v_m\cos\theta_x + w_m\sin\theta_x. \tag{6}$$

Therefore,

$$u_m = \tan\theta_x[-\mathrm{V}(\mathrm{Rx})/\sin\theta_x + V(\mathrm{Tz})], \tag{7}$$

where the angles θ_x and θ_y were determined from the measurements of the distances between transducers and the acoustic travel time relating to each bin location.

The position of each velocity reading for this work was taken as the center of the range cell, although a more accurate approach of modeling the center of the intersecting beam patterns may be investigated in the future (Zedel and Hay 2002). Small measurement inaccuracies in the positions of the transducers relative to each other could easily contribute to errors in the geometrical transformation at this stage, and it would be preferable in future work to use a precision-made jig to mount the transducers and eliminate such positioning uncertainty.

3. Experimental and field conditions

The triple-axis CDVP was deployed from a jack-up barge in a tidal inlet in the Algarve, Portugal, as shown in Fig. 3a. The inset shows the location of the field site. Figure 3b shows the alignment of the jack-up barge to the current and wave directions and the x, y, z coordinate system. The instruments were aligned into the tidal flow direction, and the wave direction was at approximately 45° to the current flow, as shown by the arrows.

The CDVP instrument was attached to the Proudman Oceanographic Laboratory (POL) Instrument Package (PIP) together with acoustic backscatter transducers, ADVs, electromagnetic current meters, and pressure sensors (Williams et al. 2003a). The instrumented PIP is shown in the photograph in Fig. 4, and the spacing between each transducer is listed in Table 1. The notations ADV-N and ADV-S represent the Nortek and Sontek ADVs, respectively. The instrumentation frame was designed to be mounted on the jack-up barge in the tidal inlet and configured to have the main instrumentation and measuring volumes 0.5 m upstream from the main support frame, pointing into the combined wave–current flows to minimize interference to the flow measurements.

The ADV instruments were located at approximately 0.15 and 0.22 m above a flat bed and measured velocities at 25 Hz. The triple-axis CDVP was located approximately 0.8 m above the bed and recorded velocity measurements at 16 Hz in 0.05-m range bins. Owing to the vertical beamwidth of the receiving transducers, the

(a)

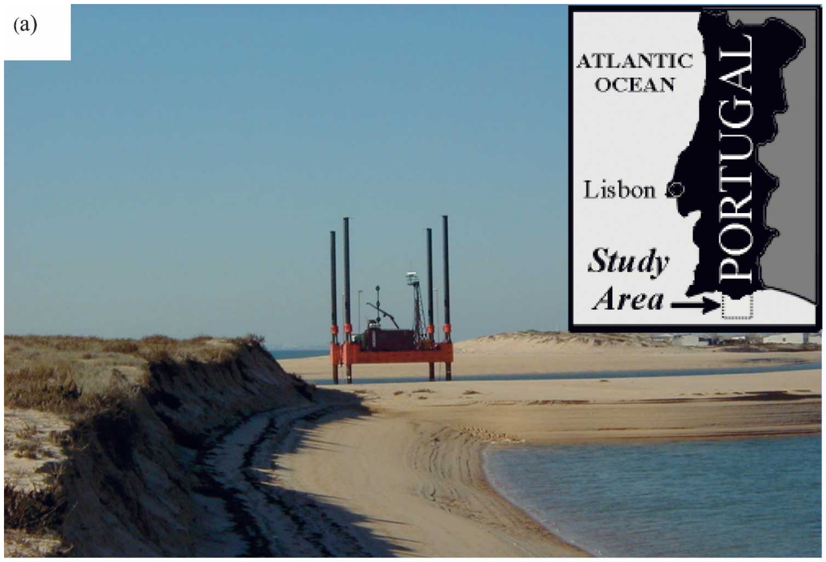

(b)

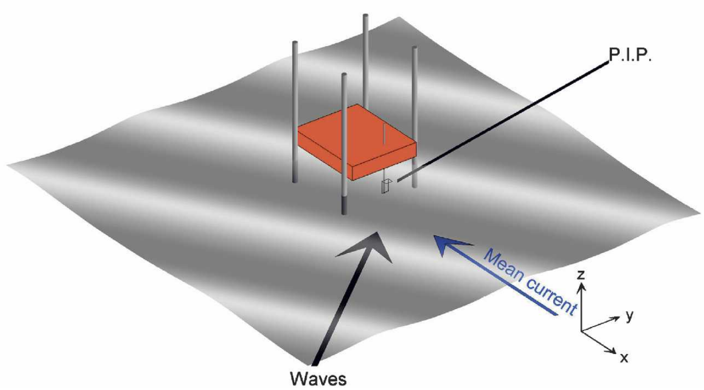

FIG. 3. (a) A photograph of the barge used to mount the instruments in the tidal inlet, with the location of the field site in the Algarve shown in the inset. (b) The diagram of the PIP relative to the current and wave directions, and the orthogonal axes x, y, and z.

first receiver range bin with overlapping u, v, and w measurements was at 0.66 m above the bed. Data from the Doppler profiler at the range bins coincident with the ADV measurement volumes were compared with the velocities measured by the two ADVs. The ADVs' velocity measurements were used as a reference to assess the CDVP at its present stage of development. The acoustic instruments were spaced apart on the frame to minimize interference between them. Owing to the main flow being in the negative x direction, it was considered that the observed flow would be only marginally modified by the instrument package (Williams et al. 2003b), and any modifications to the flow that did occur would have the same impact on the CDVP and ADV measurements.

As noted above, the instruments were aligned such that the x axes of the velocity-measuring devices were directed into the main direction of the tidal flow. As shown in Fig. 3b, the convention taken was that the streamwise flow was denoted u, measured in the x direction, with positive flow being taken as flow toward the instruments (i.e., in the negative x direction), the crosswise flow component was denoted v, in the y direction, and the vertical flow, w, was measured in the z direction. A diagram showing the relative locations of the triple-axis CDVP and the two ADVs is shown in Fig. 5. Distances between each instrument are summarized in Table 1. It should be noted that there were streamwise displacements of 0.405 and 0.525 m between the measurement volumes of ADV-N and ADV-S, re-

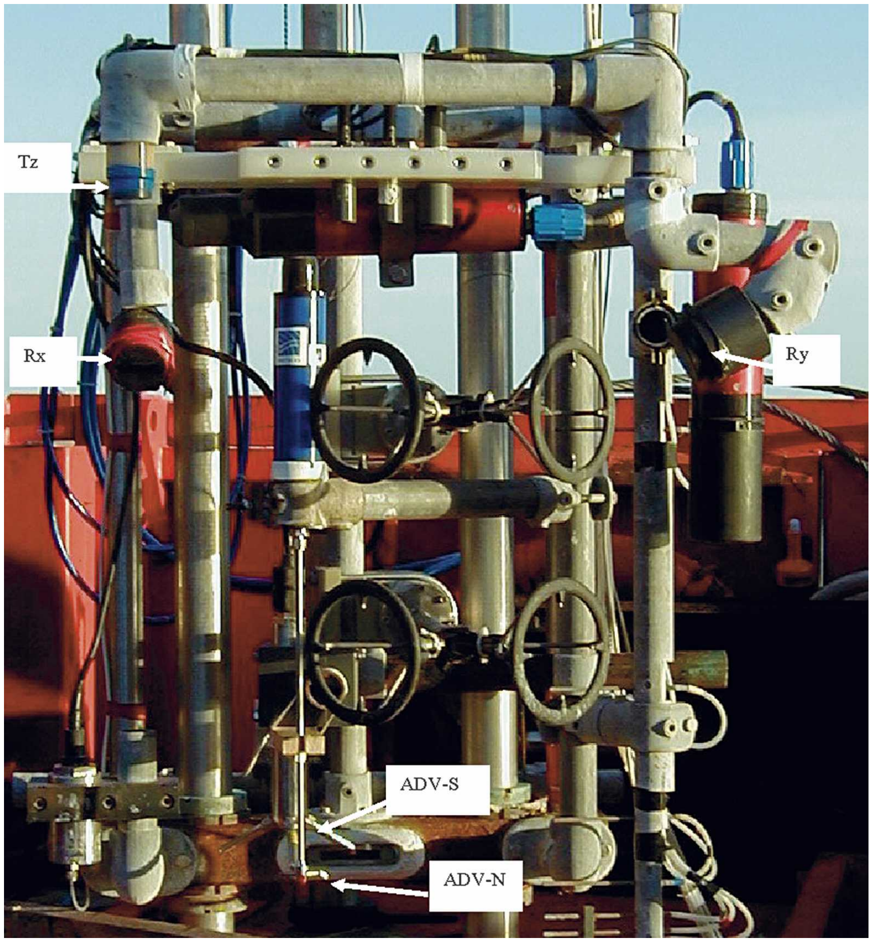

FIG. 4. Photograph of the instrument frame that was deployed for the fieldwork. The components of the triple-axis CDVP and the two ADVs are indicated.

spectively, and the CDVP, and a displacement of 0.185 m between both ADV measurement volumes and the CDVP. This impacted on the coherence of the velocities recorded by the different instruments, as discussed later.

TABLE 1. The displacement in the three orthogonal directions between the ADV measurement volumes and the transmitting and receiving transducers of the triple-axis CDVP, as shown in Fig. 5.

Measurement volume	x (m)	y (m)	z (m)
ADV-S-Tz	0.525	0.185	0.80
ADV-S-Rx	0.060	0.185	0.77
ADV-S-Ry	0.525	0.475	0.75
ADV-N-Tz	0.405	0.185	0.70
ADV-N-Rx	0.180	0.185	0.67
ADV-N-Ry	0.405	0.475	0.65
ADV-N-ADV-S	0.12	0	0.10

The field site consisted of a mobile bed of coarse sand, mean diameter $d_{50} = 1.2$ mm, with migrating bedforms of nominal height and wavelength of 0.1 and 1.0 m. Pumped sample measurements showed that the suspended sediment size varied from about 200 to 500 μm, and suspended sediment concentrations were between 0.005 and 0.5 kg m^{-3}. To demonstrate the capabilities of the triple-axis CDVP, data obtained on 28 February 1999 were selected. Data collection spanned a period of 4 h during a flood tide. On this day, $H_s \approx 0.75$ m and $T_p \approx 5$ s, and the mean current speed varied from 0.4 to 2 m s^{-1} and the water depth from 2 to 3.5 m.

4. Results

To assess the capability of the profiling Doppler system in the field, a comparison of the results obtained with the triple-axis CDVP and the two ADVs has been made. The velocity data from the CDVP and the ADV

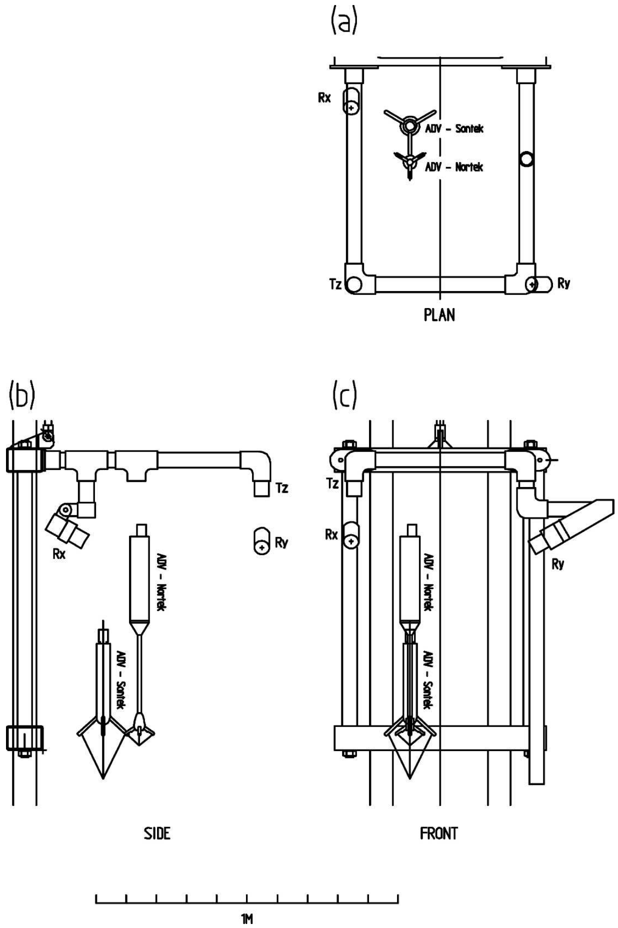

FIG. 5. Diagram of the location of the instruments on the frame: (a) plan view in the (x, y) plane, (b) side view in the (x, y) plane, and (c) front view in the (y, z) plane. The relative positions are given in Table 1.

were corrected for misalignment relative to the main flow in the vertical and horizontal planes using a rotation matrix,

$$\mathbf{T} = \begin{pmatrix} \cos\varphi & -\sin\varphi \\ \sin\varphi & \cos\varphi \end{pmatrix},$$

where for a rotation about the z axis, φ is the angle between the mean data and the x axis. The velocities u_1 and υ_1 of the rotated data were thus

$$\begin{pmatrix} u_1 \\ \upsilon_1 \end{pmatrix} = \mathbf{T}\begin{pmatrix} u_m \\ \upsilon_m \end{pmatrix},$$

where u_m and υ_m are the measured velocities. Similarly,

$$\begin{pmatrix} u \\ w_1 \end{pmatrix} = \mathbf{T}\begin{pmatrix} u_1 \\ w_m \end{pmatrix} \quad \text{and} \quad \begin{pmatrix} \upsilon \\ w \end{pmatrix} = \mathbf{T}\begin{pmatrix} \upsilon_1 \\ w_1 \end{pmatrix}.$$

The data u, υ, and w were the final rotated velocities for zero-mean cross and vertical flow. The measured and rotated data are plotted in Fig. 6, showing the angle, φ

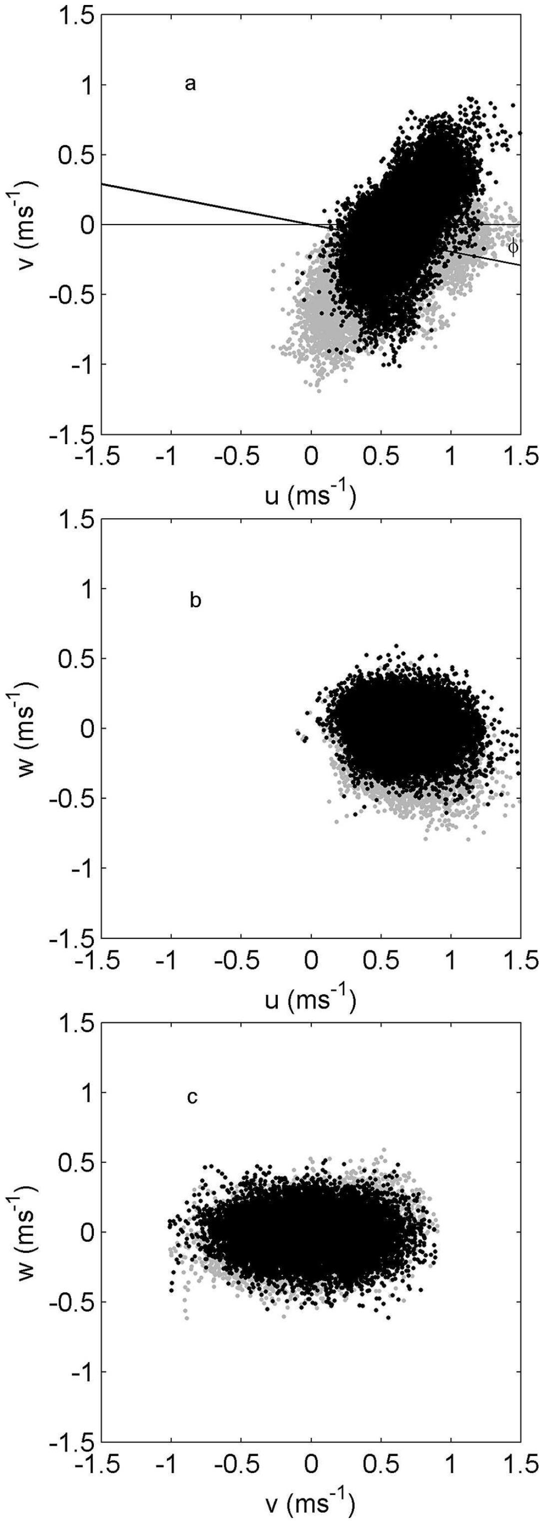

FIG. 6. Depiction of how the data were rotated to correct for misalignment relative to the main flow in the vertical and horizontal planes. (a) The measured (u_m and υ_m) and rotated (u and υ) velocity data plotted in gray and black, respectively. Similarly, shown are (b) υ and w, and (c) u and w. The rotation angle, φ, is marked in (a).

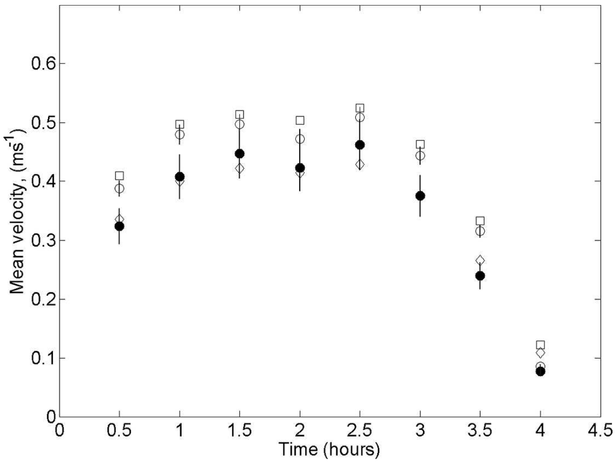

FIG. 7. Plot showing the mean current measured by the CDVP and also the two ADVs over a 3.5-h time period. The CDVP velocity measurements shown are at nominal heights above the bed of 0.07 m (●) and 0.18 m (○). These range bins were the closest to the measurement volumes of the ADVs, at nominal heights of 0.08 m (◊) and 0.18 m (□), respectively, above the bed.

$= \tan^{-1}(\langle v\rangle/\langle u\rangle)$, where $\langle\rangle$ denotes the mean. The rotation was applied to each dataset to obtain the flow parallel to the bed.

a. Comparison of CDVP and ADV time-averaged velocity measurements

The triple-axis CDVP recorded velocity measurements at 16 Hz, and the ADV instruments at 25 Hz; however, an initial comparison of the measurements was made using the measured mean velocity. The mean was obtained over the recording interval of 1024 s for the instruments, over a 4-h flood period. The range bins of the CDVP closest to the ADVs were chosen for the comparison. These occurred at 0.07 and 0.18 m above the average bed location for the ADV-S and ADV-N, respectively. The mean velocities recorded for the three instruments are plotted over a flood cycle in Fig. 7. The error bar in the CDVP measurement is based on the difference in the velocities between two adjacent range bins, this being approximately equivalent to the difference in velocity, which would be measured at the top and the bottom of each range bin due to the length of the range bin, approximately 0.05 m. Within the error bars on these measurements, the plot in Fig. 7 shows that there is agreement in the mean streamwise flow velocity measured by the CDVP and both ADVs. Using a normal axis regression to compare the data gave a regression gradient of 0.96 ± 0.06 for the comparison with the ADV-N, with a regression coefficient of 0.999, and a gradient of 1.02 ± 0.11 for the ADV-S, with a regression coefficient of 0.998. Testing the significance of the gradient using the t-distribution value gave $t = 0.667$ and $t = 0.182$ for the ADV-N and ADV-S data, respectively, which was less than the 1% t-distribution value of 3.7 for $n = 8$. The regression gradients therefore did not differ significantly from unity at the 99% confidence level.

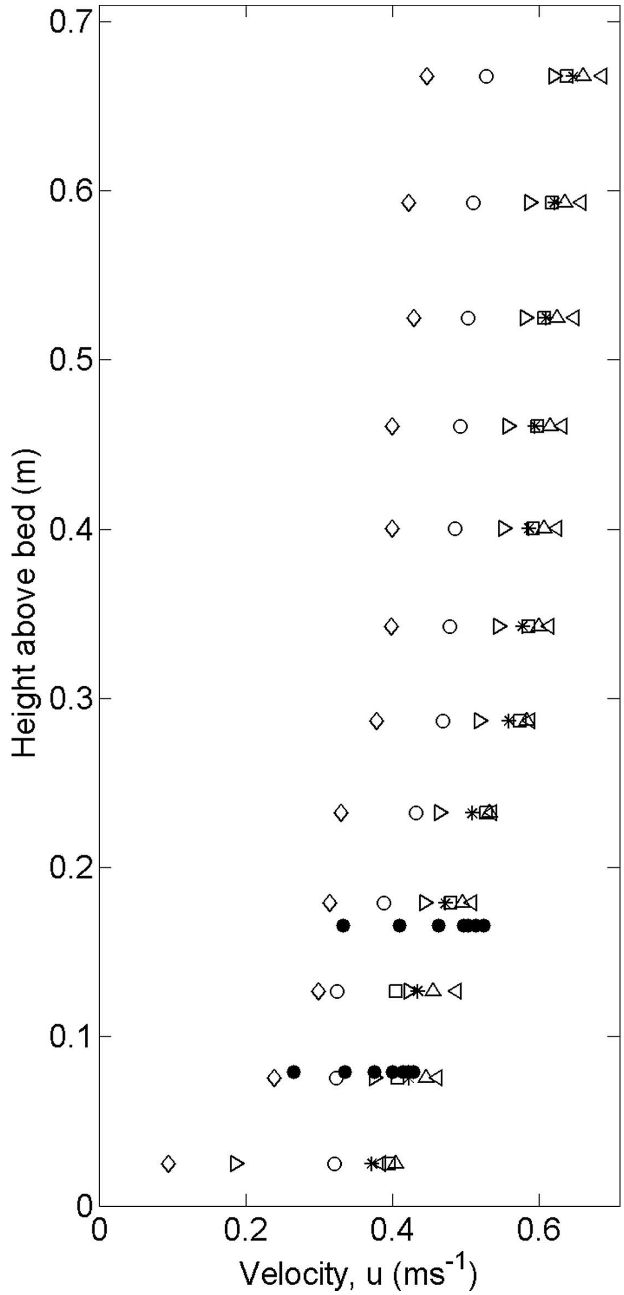

FIG. 8. Velocity profile measured by the CDVP over a flood cycle from 0959 to 1359 UTC (o for 0959, □ for 1029, △ for 1059, * for 1129, ◁ 1159 ▷ for 1229, and ◊ for 1359 UTC). The different symbols enable the shape of the velocity profiles to be distinguished over the tidal cycle. The measurements obtained with the ADVs are also shown (●).

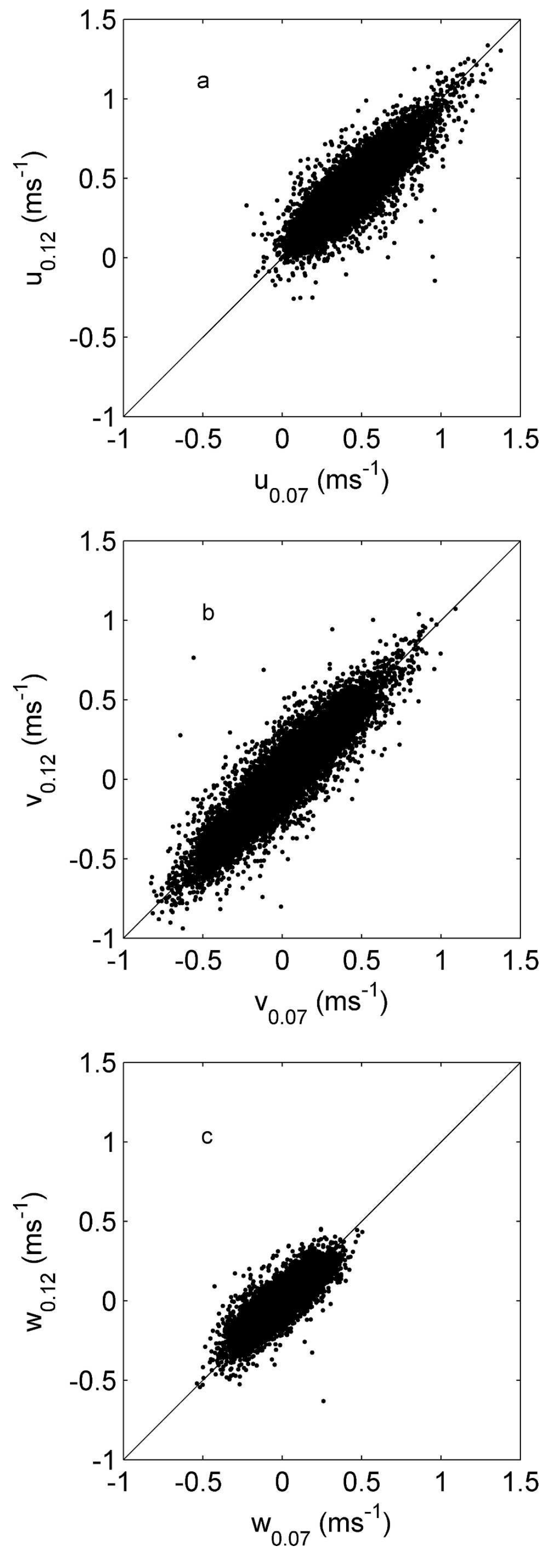

FIG. 9. Scatterplots showing the regression of velocities measured in adjacent CDVP range bins, at 0.07 and 0.12 m above the bed, $Vi_{0.07}$ vs $Vi_{0.12}$, where Vi is (a) u, (b) v, and (c) w. The regression data for these heights and two other adjacent bin heights are given in Table 2.

TABLE 2. Mean regression gradients and coefficients for the comparison between the velocities measured in adjacent CDVP range bins. The mean was taken over the eight records of data throughout the tidal cycle.

	CDVP at heights 0.59 and 0.67 m	CDVP at heights 0.34 and 0.40 m	CDVP at heights 0.07 and 0.12 m
Regression gradient u	0.98 ± 0.01	0.98 ± 0.01	0.95 ± 0.06
Regression coefficient u	0.99 ± 0.004	0.99 ± 0.002	0.97 ± 0.02
Regression gradient v	0.99 ± 0.2	0.97 ± 0.002	0.80 ± 0.3
Regression coefficient v	0.97 ± 0.008	0.96 ± 0.004	0.75 ± 0.2
Regression gradient w	0.99 ± 0.02	1.03 ± 0.03	0.67 ± 0.5
Regression coefficient w	0.91 ± 0.02	0.86 ± 0.03	0.45 ± 0.17

b. *Time-averaged velocity profiles*

The triple-axis CDVP had the capability to measure the velocity in range bins of approximately 0.05 m over a 1.28-m range. In the present study the CDVP was mounted at 0.8 m above a mean bed location, though the actual height of the range bins above the bed varied over the measurement period due to the migration of bedforms below the instrument package. The range to the bed was determined by identifying when bed echoes contaminated the data. Figure 8 shows the mean streamwise velocity profiles, measured by the triple-axis CDVP over the flood period. These profiles show an increase in velocity with increasing height above the bed, with the velocities approaching zero toward the bed, as would be expected. Some detailed variations in the shape of the velocity profiles were observed over the flood, which was considered to be partly due to the migrating bedform beneath the instruments.

c. *Intercomparison of Doppler range bins*

Each backscattered range bin signal provided an independent measurement of velocity, and adjacent range bins would be expected to measure very similar velocities if the measurements were internally consistent. It was therefore considered judicious to compare time series of velocities from several adjacent range bins and to assess the internal veracity of the CDVP measurements. Data from adjacent range bins near to the bed, in the middle of the velocity profile and higher in the water column, were compared for each of the 1024-s records collected over the tidal cycle. An example of the scatterplots obtained for the 16-Hz data between adjacent range bins is shown in Fig. 9. This

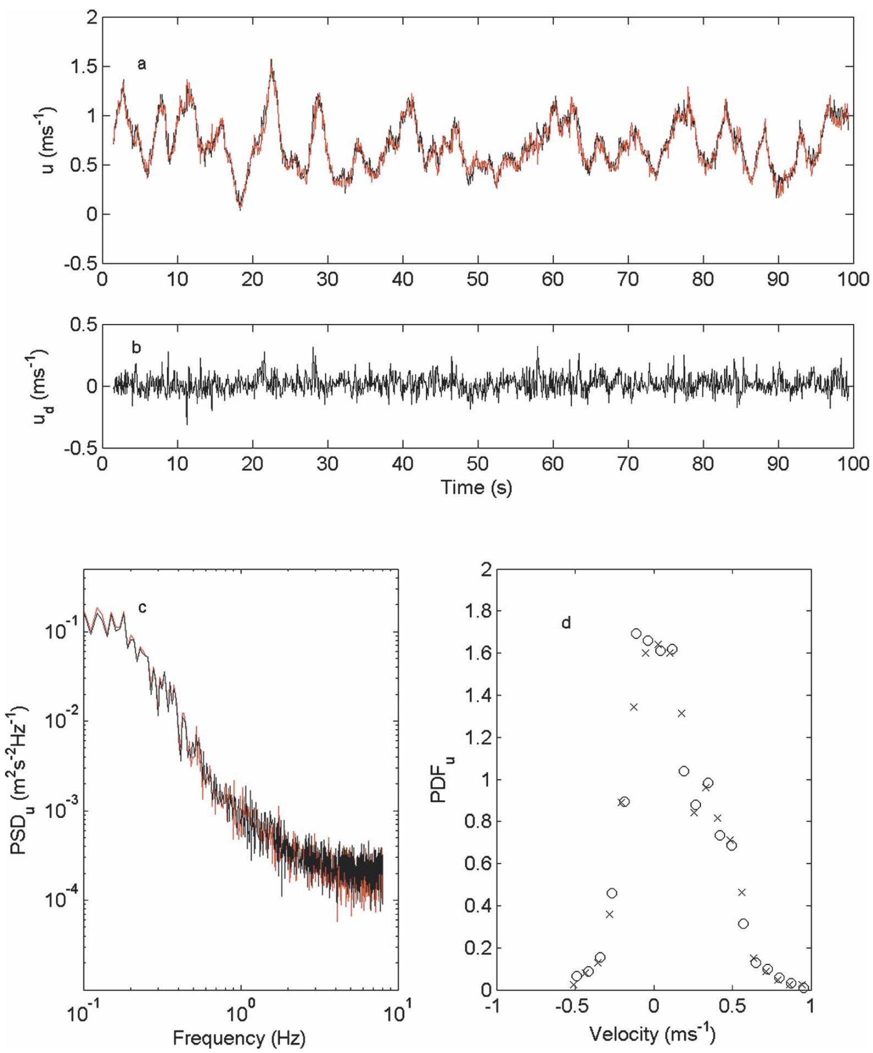

FIG. 10. Plots showing a comparison of the streamwise flow, u, measured between two adjacent range bins at nominally 0.34 m (red) and 0.40 m (black) above the bed. (a) The velocities measured at 16 Hz by the triple-axis CDVP. (b) The difference in these velocities. (c) The power spectra of the zero-mean u velocities. (d) The probability density functions of the zero-mean velocities for 0.34 m (x) and 0.40 m (o).

shows u, v, and w from range bins at 0.07 and 0.12 m above the bed for one record. Although there is some scatter in the data associated with detailed differences in the higher-frequency velocity components, the data are clearly clustered around the line of gradient unity shown in the figure. To assess such results as shown in Fig. 9 the mean regression data from all the records at three heights above the bed are given in Table 2. The table shows regression gradients close to unity and regression coefficients generally greater than 0.9. In each case the dependent variable was taken as the lower of the two bins; hence the gradients are generally slightly less than unity. The gradients approach unity higher up the water column, which is consistent with the shape of the velocity profile. Figures 10 and 11 show further examples of the results obtained from intercomparison of range bins at 0.34 and 0.4 m above the bed. The figures show typical velocity time series, power spectral density, and probability distribution plots for the u and w velocities for one record. The intercomparison of v was similar to that of u and is therefore not shown for brevity. Figure 10a shows an example of 100 s of time series velocity data for the adjacent range bins. As can be seen, the velocities are very comparable. Figure 10b shows the velocity difference between the two bins. To quantify the difference, $\langle|\zeta_d|\rangle/\tilde{u}$ was calculated, where $\langle|\zeta_d|\rangle = \langle|\zeta_i - \zeta_j|\rangle$, ζ represents u, v, or w; i and j represent adjacent range bins, $\tilde{u} = \langle(|u_i| + |u_j|)\rangle/2$; and $\langle\rangle$ repre-

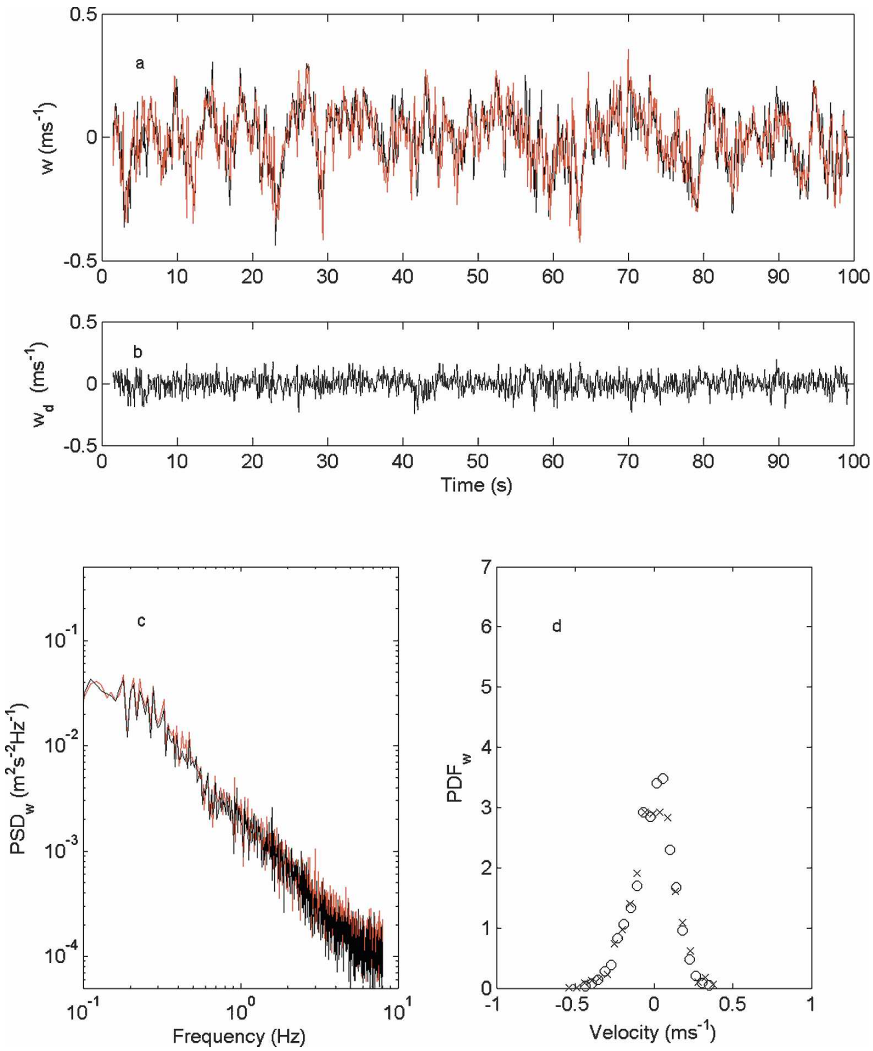

FIG. 11. As in Fig. 10, but for w.

sents an average over a record. The average for $\langle|\zeta_d|\rangle/\tilde{u}$ over the flood period gave values of 0.09 ± 0.02 and 0.10 ± 0.02 for u and υ, respectively. This was considered acceptable owing to the 0.06-m vertical separation in the measurement volumes and the probable spatial decorrelation of the higher-frequency velocity components. Figures 10b and 10c show the power spectral density and the probability density function for the velocities. As can be seen, the adjacent range bins gave very comparable results. Figure 11 shows the results from the two range bins for w. As with Fig. 10, the time series, spectra, and probability distributions are seen to be very comparable, with a value for $\langle|\zeta_d|\rangle/\tilde{u} = 0.09 \pm 0.015$, which is similar to the values for u and υ.

d. Comparison of ADV velocities

Before making a comparison of the CDVP with the two ADV instruments, it was considered useful to assess the coherence of the velocities measured by the two ADVs. The ADV-N and the ADV-S were separated vertically by 0.1 m and horizontally in the x direction by 0.12 m. Although a number of analyses were conducted, the main outcome can be illustrated by the results in Figs. 12a–c. These scatterplots show measurements for u, υ, and w. Regression analysis gave gradients and coefficients of 1.20 ± 0.01 and 0.97 for u and 1.09 ± 0.03 and 0.93 for υ. The gradients are greater than unity due to the ADV-N, the ADV farthest from the bed, being the dependent variable. For w the comparable results were a gradient of 0.8149 and a regression coefficient 0.133, the latter being significantly below those for u and υ. This relatively weak correlation in w was considered to be due to the reduced coherency owing to horizontal and vertical separation of the ADVs. Calculation of $\langle|\zeta_d|\rangle/\tilde{u}$ gave mean values over the flood for u and υ of 0.17 ± 0.01 and 0.16 ± 0.01, re-

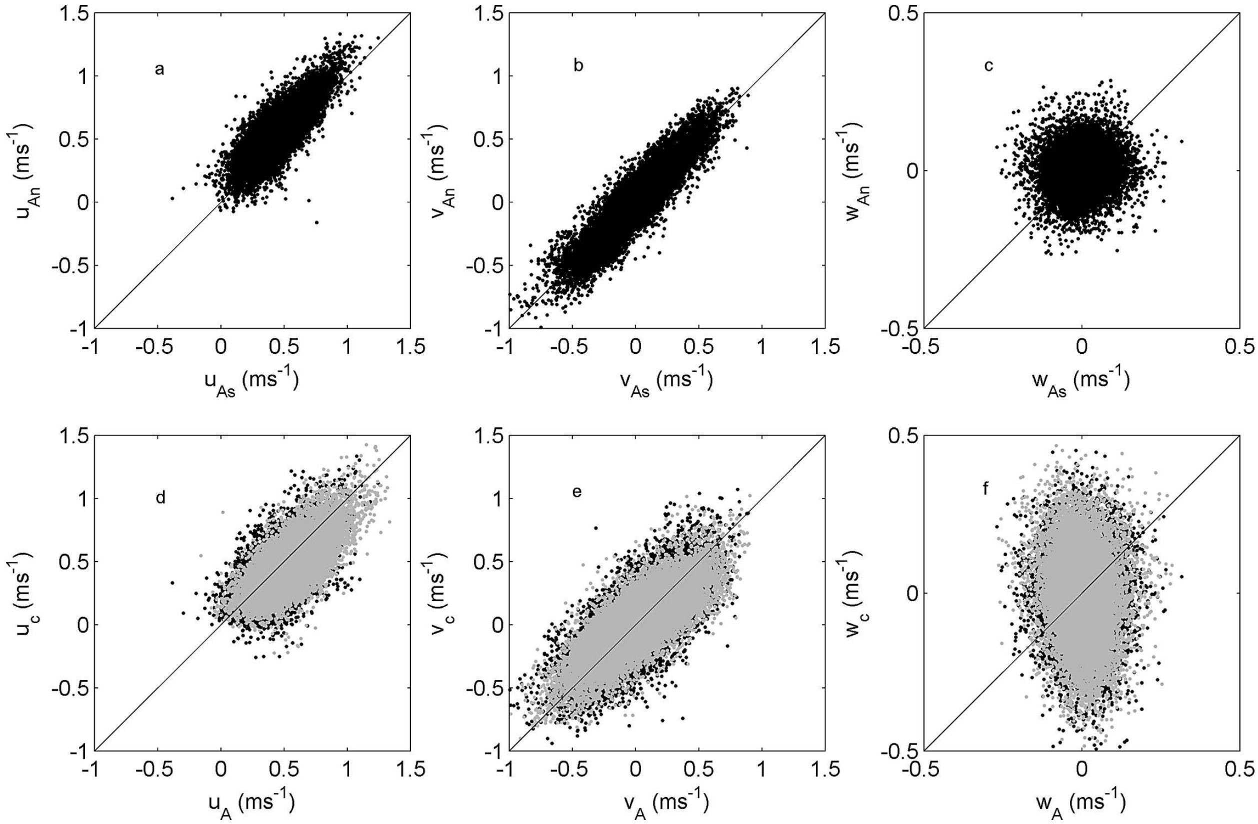

FIG. 12. Plots of the regression of ADV-S Vi vs ADV-N Vi, where Vi is (a) u, (b) v, and (c) w; and scatterplots of ADV-S Vi vs CDVP Vi (black) and of ADV-N Vi vs CDVP Vi (gray), where Vi is (d) u, (e) v, and (f) w.

spectively. These values are somewhat larger than calculated for the CDVP adjacent range bin analysis, which is ascribed to the vertical and horizontal separation of the ADVs.

e. Comparison of the CDVP with the ADV at 16 Hz

Figure 12 is used as the starting point for this section. Figures 12d–f show scatterplots of the velocity for the CDVP versus the ADVs. The scatterplots in Figs. 12d–f are comparable with those in Figs. 12a–c, with the u and v data for the CDVP versus that for the ADVs being clustered about the line of gradient unity and with obvious correlation, and with almost no correlation for the w component of flow. This lack of correlation for the w component is ascribed to the horizontal spatial separation of the CDVP and the ADVs. Both of the ADVs were displaced 0.185 m in the y direction, crosswise, and 0.405 and 0.525 m in the x direction, streamwise, respectively, for ADV-N and ADV-S from the CDVP measuring volume. Conducting a linear regression on the 16-Hz CDVP and ADV data gave the results shown in Table 3. These were obtained by carrying out a linear regression on each of the 1024-s records over the flood period and forming the mean and standard deviation for the gradient and regression coefficient. For the u component of flow, the results show gradients marginally less than unity, although with standard deviations that encompass unity, and high regression coefficients. The departure of the gradients from unity could be associated with the bed level and local bedforms. Although the range bins corresponding to the ADVs' measurement volumes remained fixed, the height of both the CDVP range bins and ADVs' measurement volumes varied with height above the bed within a record and from record to record due to migrating bedforms below the instruments. For the v component, the gradients are below unity and with reduced regression coefficients. This may in part be due to the difference in measurement heights, as noted above, and in some manner associated with spanwise decorrelation of the v component, as expressed by the reduced regression coefficients; however, at present this difference is not fully resolved. The w component of flow shows no correlation, which is ascribed to the spatial decorrelation of the 16-Hz ve-

TABLE 3. Mean regression gradients and coefficients for the comparison between the ADV and CDVP velocity measurements. The mean was taken over the eight records of data throughout the tidal cycle.

	CDVP/ADV-S	CDVP/ADV-N
Regression gradient u	0.95 ± 0.09	0.90 ± 0.09
Regression coefficient u	0.90 ± 0.06	0.95 ± 0.03
Regression gradient v	0.80 ± 0.3	0.72 ± 0.2
Regression coefficient v	0.63 ± 0.2	0.69 ± 0.2
Regression gradient w	12 ± 23	10 ± 26
Regression coefficient w	-0.002 ± 0.08	-0.1 ± 0.12

locity time series, as discussed above in reference to Fig. 12f.

Figures 13–15 show typical examples of CDVP and ADV time series, power spectral density, and probability density function plots for the three components of velocity. Since the comparison of the CDVP with the two ADVs gave very similar results, only those with the ADV-N are shown for brevity. The u and the v components presented in Figs. 13 and 14 show CDVP results that compare very favorably with the ADV measurements, having time series, spectra, and probability distributions in general agreement. There are differences in the spectrum: the CDVP spectra begin to de-

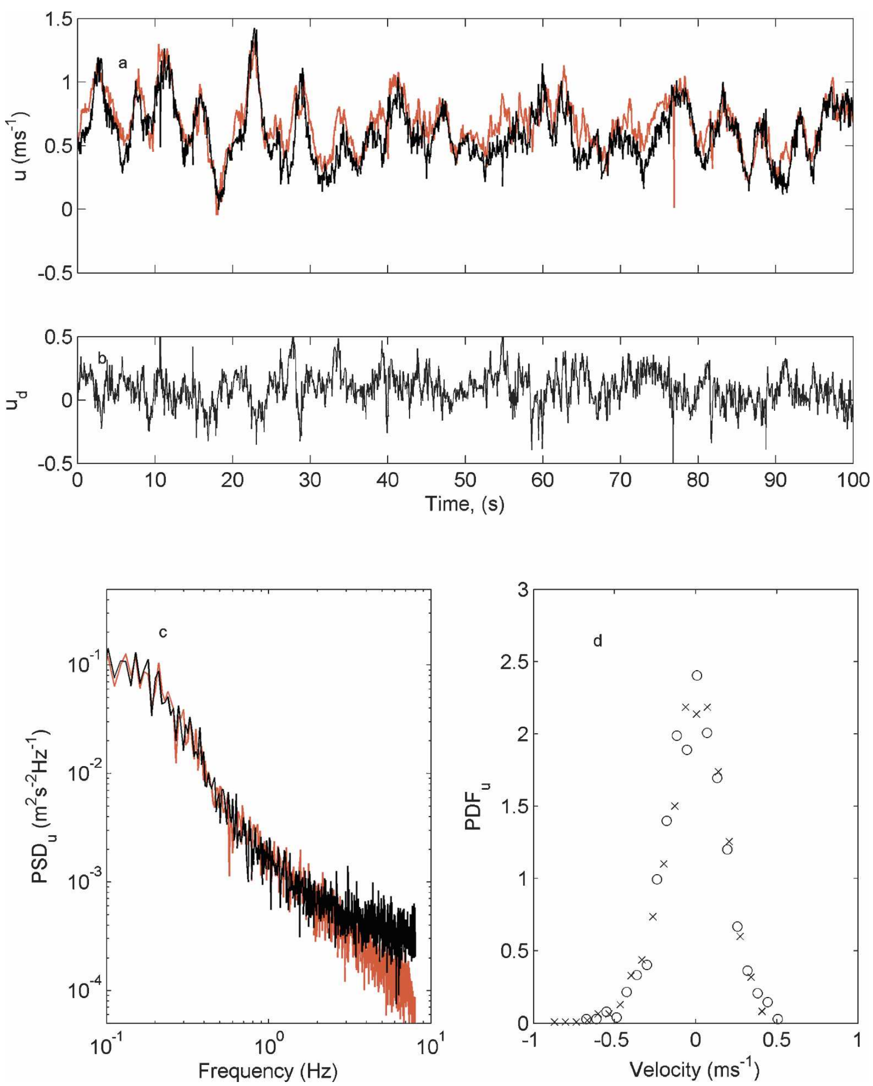

FIG. 13. Plots showing a comparison of the streamwise flow, u, measured by the ADV-N (red) and the CDVP (black). (a) The velocities measured at 16 Hz. (b) The difference in these velocities. (c) The power spectra of the zero-mean u velocities. (d) The probability density functions of the zero-mean velocities for the ADV-N (o) and the CDVP (x).

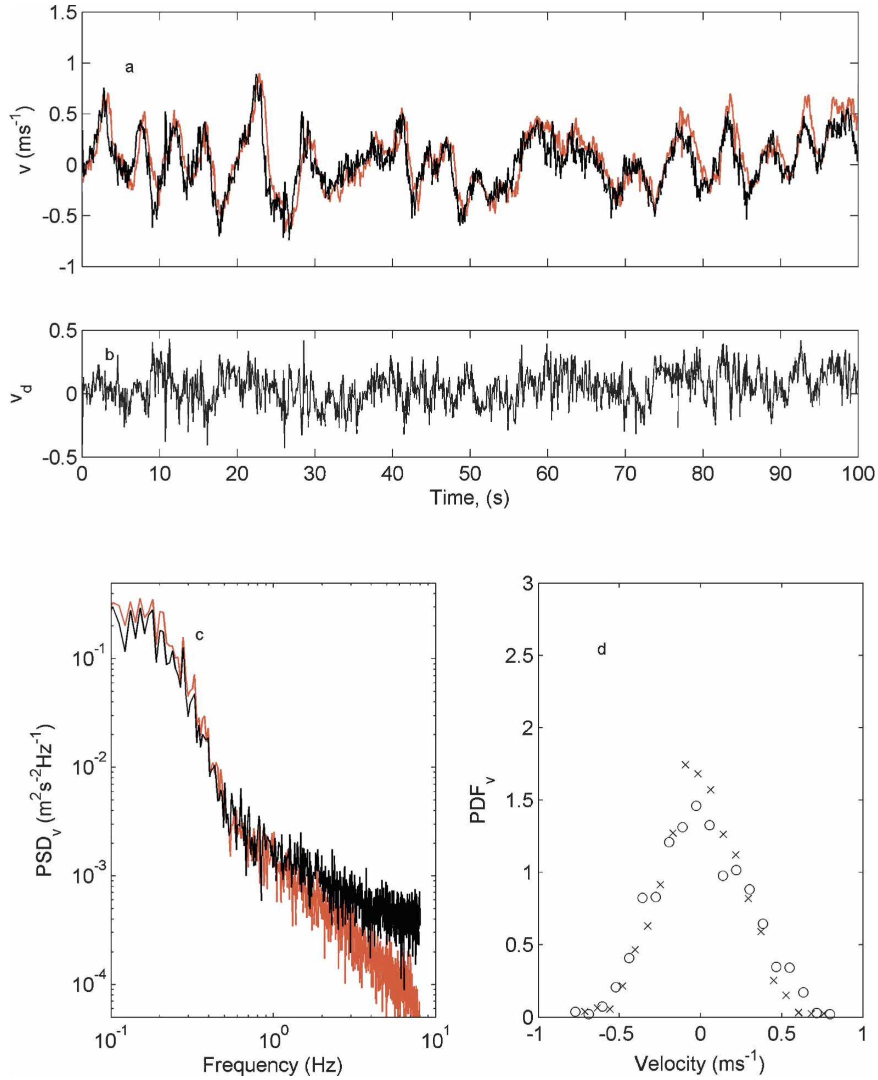

FIG. 14. As in Fig. 13, but for v.

part from the ADV above about 4 Hz, with the CDVP measuring larger spectral components at the higher frequencies. This trend was common to all the records and may be a limitation of the present CDVP system. The mean values for $\langle|\zeta_d|\rangle/\tilde{u}$, averaged over the flood, were 0.24 ± 0.02 and 0.28 ± 0.03 for u and v, respectively. These values for $\langle|\zeta_d|\rangle/\tilde{u}$ are larger than observed in the comparisons between adjacent CDVP bins, though not much greater than the ADV intercomparison; it is therefore considered that the spatial separation of the ADVs from the CDVP range bins could readily account for the increase in $\langle|\zeta_d|\rangle/\tilde{u}$. The comparison of the w component of flow is less convincing, as can be seen in Fig. 15. From the discussions above, detailed time series comparisons were expected to be problematic, given the negligible regression coefficient. However, it was anticipated that the form of the spectra and the probability distribution would give comparable results. As can be seen in Fig. 15c, the spectra are comparable in form, though the CDVP is showing substantially larger spectral components at the lower frequencies; also, the probability distribution shown in Fig. 15d has CDVP velocities spread over a greater range of velocities than the ADVs. These differences may possibly be ascribed to bedform effects (Williams et al. 2003b) or may be due to residue components of u and v, after the rotation transformation, still partially contaminating w.

f. Visualization of the wave and turbulent flow

Figure 16, which illustrates the capability of the CDVP for visualizing the flow, is a plot of the velocity

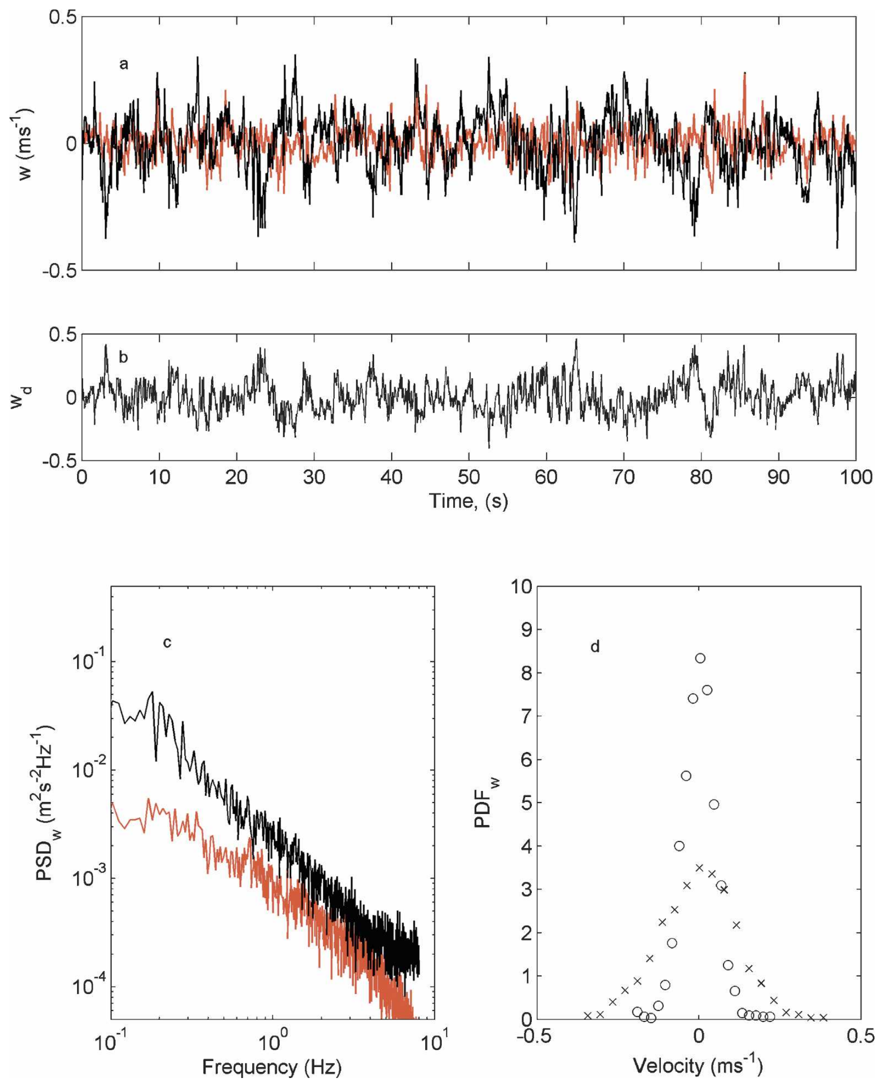

FIG. 15. As in Fig. 13, but for w.

vectors, including wave and turbulent components. The figure shows the u–w, v–w, and u–v velocity vectors, where the individual velocity components were zero meaned, plotted over a 5-s time period, between 0.05 and 0.7 m above the bed. The length of the velocity vectors is indicated in the figure. A single-point-measurement instrument such as an ADV can provide the time-varying velocity vectors at a single height above the bed; however, the spatial profiling that is achievable with the triple-axis CDVP provides a capability to visualize structures in the flow. Such structures, which can be seen in Fig. 16, are probably associated with the wave component of the flow. This type of plot exemplifies the value of developing a three-axis CDVP with collocated volumes, since it clearly illustrates the finescale temporal and spatial flow structures that can be measured in the near-bed flow regime.

5. Discussion and conclusions

The aim of the present paper was to report on an assessment of a three-axis CDVP that is under development. The advantage of the present system over commercially available coherent Doppler profiling systems is that the measurement volumes for u, v, and w are coincident. The collocation of the velocity measurement volume is an essential requirement for many hydrodynamic and sediment process studies. The first trial of the instrument was in a field campaign at a coastal lagoon inlet in Portugal. As part of the campaign an instrument package was deployed to investigate near-bed sediment processes, and advantage was taken of this study to deploy the CDVP and pragmatically assess its capability in a marine setting.

To assess the CDVP, velocities were compared from

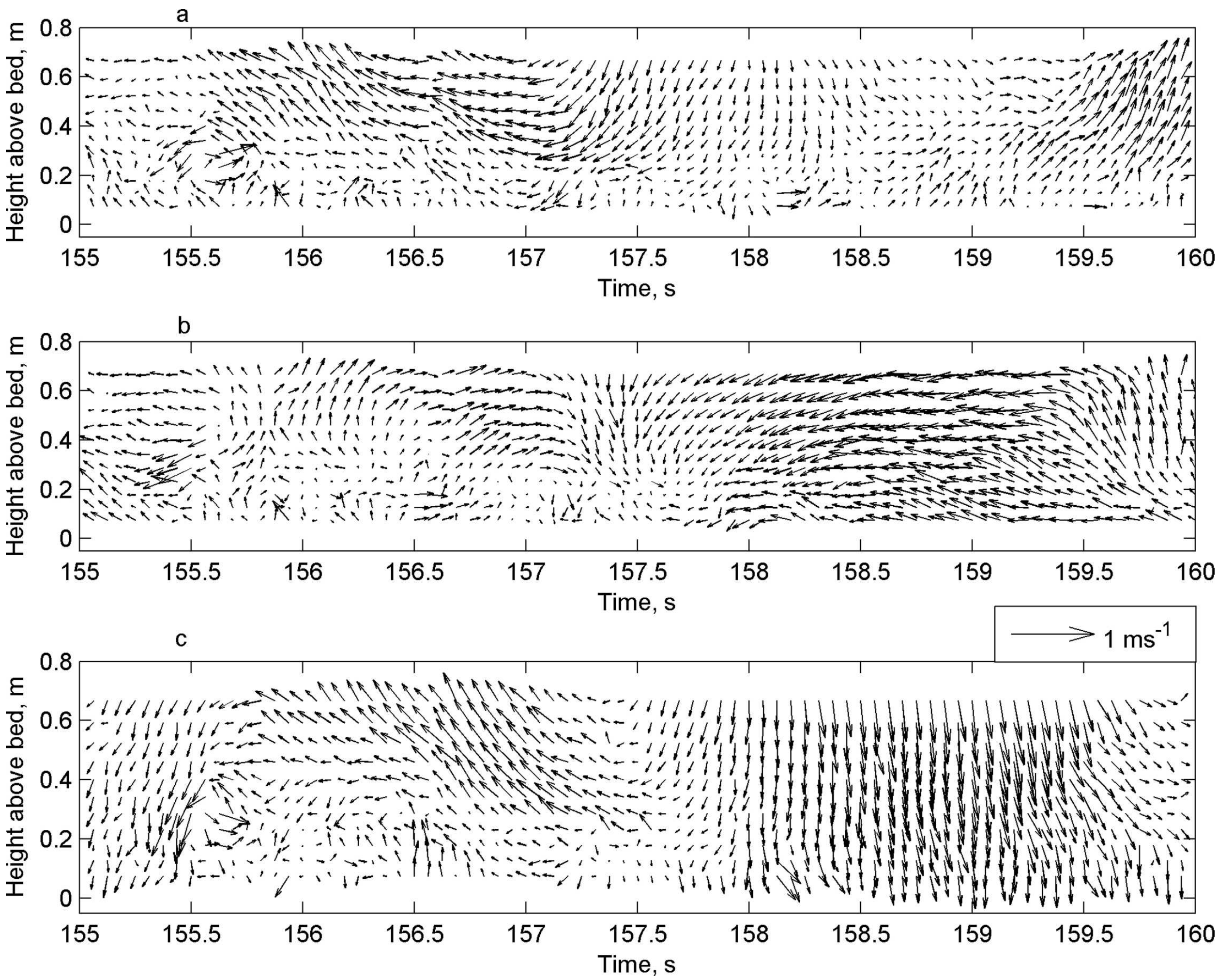

FIG. 16. Plot demonstrating the capability of the triple-axis CDVP to aid with the visualization of the wave and turbulent flow. Plots (a), (b), and (c) show a time series over a 5-s period of the zero-mean velocities displayed as vectors *u*–*w*, *v*–*w*, and *u*–*v*, respectively. The vertical scale covers the range measured by the profiler in 0.05-m steps above the bed.

independent adjacent range bins to examine the internal consistency of the CDVP, and two commercially available instruments, ADVs, were used as the reference instruments against which the CDVP's performance was gauged. Initial comparisons of the streamwise mean velocities of the tidal current over a flood period produced encouraging results, with CDVP and ADV measurements showing no significant difference. Following the mean measurements, the 16-Hz CDVP was examined by comparing the observations from adjacent range bins. Linear regression, time series comparisons and differences, power spectral densities, and probability distribution functions were used to assess the internal consistency of the measurements. These comparisons showed that adjacent range bins yielded very comparable results, thereby establishing the internal consistency of the CDVP measurements. Comparison of the 16-Hz CPVP measurements with the ADV observations was also carried out using linear regression, time series comparisons and differences, power spectral densities, and probability distribution functions. This comparison was hindered to some extent by the spatial separation of the ADVs and the CDVP measurement volumes and by the variable height of the measurement volumes above the bed due to bedform migration. However, with this caveat a comparison was conducted. The results showed very comparable measurements for u, comparable observations for v, and poor agreement for w. Two observations on the u, v, CDVP comparisons with the ADV were that the regression plots yielded gradients less than unity, and the power spectra for the CDVP appeared to be reaching a noise floor above about 4 Hz. The reduced gradients for u, 0.95 ± 0.1 and 0.90 ± 0.1, were considered to be possibly due to the spatial separation and local bed-height variation; however, the lower gradients for v, 0.80 $\pm$ 0.3 and 0.72 $\pm$ 0.2, were not so readily reconciled. The flattening off of the power spectral density above about 4 Hz may be a limitation of the system at the present stage of development. The w components of the CDVP and the ADVs were temporally uncorrelated, which was unsurprising given the spatial separation and the results from the intercomparison of the two ADV measurements. What were more difficult to explain were the differences in the power spectral density and probability density function, which seemed to be indicating some contamination of the vertical component of the flow by the horizontal components.

Although the present assessment of the triple-axis CDVP is to some extent limited by the lack of collocation of the ADV and CDVP measuring volumes, it is nevertheless considered worthwhile to take advantage of the experimental setup to assess the capability of the CDVP in a marine setting. The results were generally positive and supported the concept of using acoustics to obtain nonintrusive, high-spatial- and high-temporal-resolution profiles of collocated three-axis velocity measurements in a nearshore coastal environment. It is anticipated that the CDVP, coupled with comparable suspended sediment and bedform measurements, will make an important contribution to probing hydrodynamic and sediment processes in the bottom boundary benthic layer.

Acknowledgments. The authors would like to acknowledge support from the European MAST III project Inlet Dynamics Initiative Algarve (INDIA) (Contract MAS3-CT97-0106) and the Natural Environment Research Council. The authors thank Marine Electronics, Ltd., for their assistance and Peter Hardcastle for the electronics developments. Thank you to the reviewers for interesting questions and suggestions. Thanks also to Alex Souza for helpful discussions.

REFERENCES

Betteridge, K. F. E., P. D. Thorne, and P. S. Bell, 2002: Assessment of acoustic coherent Doppler and cross-correlation techniques for measuring near-bed velocity and suspended sediment profiles in the marine environment. *J. Atmos. Oceanic Technol.,* **19,** 367–380.

Hardcastle, P. J., 1994: A high resolution near-bed coherent acoustic Doppler current profiler for measurement of turbulent flow. *Proc. Sixth Int. Conf. on Electronic Engineering in Oceanography,* London, United Kingdom, IEE, Conf. Publ. 394, 73–76.

Hurther, D., and U. Lemmin, 1998: A constant-beam-width transducer for 3D acoustic Doppler profile measurements in open-channel flows. *Meas. Sci. Technol.,* **9,** 1706–1714.

——, and ——, 2001: A correction method for turbulence measurements with a 3D acoustic Doppler velocity profiler. *J. Atmos. Oceanic Technol.,* **18,** 446–458.

Lhermitte, R., and R. Serafin, 1984: Pulse-to-pulse coherent Doppler sonar signal processing techniques. *J. Atmos. Oceanic Technol.,* **1,** 293–308.

Rolland, T., and U. Lemmin, 1997: A two-component acoustic velocity profiler for use in turbulent open-channel flow *J. Hydro. Res.,* **35,** 545–562.

Thorne, P. D., and J. Taylor, 2000: Acoustic measurements of boundary layer flow and sediment flux. *J. Acoust. Soc. Amer.,* **108,** 1568–1581.

——, and D. Hanes, 2002: A review of acoustic measurement of small scale sediment processes. *Cont. Shelf Res.,* **22,** 603–632.

Veron, F., and W. K. Melville, 1999: Pulse-to-pulse coherent Doppler measurements of waves and turbulence. *J. Atmos. Oceanic Technol.,* **16,** 1580–1596.

Voulgaris, G., and J. H. Trowbridge, 1998: Evaluation of the acoustic Doppler velocimeter (ADV) for turbulence measurements. *J. Atmos. Oceanic Technol.,* **15,** 272–289.

Williams, J. J., P. S. Bell, J. D. Humphery, P. J. Hardcastle, and P. D. Thorne, 2003a: New approach to measurement of sediment processes in a tidal inlet. *Cont. Shelf Res.,* **23,** 1239–1254.

——, ——, and P. D. Thorne, 2003b: Field measurements of flow fields and sediment transport above mobile bed forms. *J. Geophys. Res.,* **108** (C4), 6–36.

Wilson, R. A., P. D. Thorne, J. J. Williams, P. S. Bell, and P. J. Hardcastle, 2000: An evaluation of a 3D acoustic coherent Doppler current profiler in the marine environment. *Proc. of the Fifth European Conf. on Underwater Acoustics (ECUA 2000),* Lyon, France, European Commission, 627–632.

Zedel, L., and A. E. Hay, 1999: A coherent Doppler profiler for high-resolution particle velocimetry in the ocean: Laboratory measurements of turbulence and particle flux. *J. Atmos. Oceanic Technol.,* **16,** 1102–1117.

——, and ——, 2002: A three component bistatic coherent Doppler velocity profiler: Error sensitivity and system accuracy. *IEEE J. Ocean. Eng.,* **27,** 717–725.

——, ——, R. Cabrera, and A. Lohrmann, 1996: Performance of a single beam pulse to pulse coherent Doppler profiler. *IEEE J. Ocean. Eng.,* **21,** 290–297.